Effects of interlayer coupling on the dynamic ordering of vortices in high-T_c $YBa_2Cu_3O_{7-\delta}/PrBa_2Cu_3O_{7-\delta}$ superlattices

W. K. Park and Z. G. Khim
Department of Physics, Seoul National University, Seoul 151-742, Korea
(Received 15 April 1999; revised manuscript received 9 July 1999)

We have fabricated and measured transport properties of high-T_c $\{YBa_2Cu_3O_{7-\delta}\}_8/\{PrBa_2Cu_3O_{7-\delta}(PBCO)\}_n$ $(n=2, 4, 8)$ superlattices in order to investigate the effect of interlayer coupling on the vortex dynamics. The resistive transition was analyzed based on the theory of vortex fluctuations such as the Kosterlitz-Thouless vortex-antivortex unbinding transition and two-dimensional (2D) Coulomb gas (CG) analogy of vortices. We have found out that deviation of the sheet resistance curve from the universal one of 2DCG theory increases as the intervening PBCO layer gets thinner, which can be understood as the result of a strengthened interlayer coupling. Measurements of current-voltage characteristics revealed further evidences of the vortex-antivortex unbinding transition. From noise measurements, we observed that the noise power appeared only in tail parts of resistive transition curves and was strongly dependent on both transport current and magnetic field, which implies that the vortex motion is the main source of voltage noise in these specimens. The peak value of noise power showed nonmonotonic dependence on the current, while it was suppressed monotonically with increasing field. Maximal noise peak power and the corresponding current value increased simultaneously as the PBCO layer got thicker. We could understand these behaviors using the concept of dynamic ordering of vortices, i.e., vortex motion becomes more independent of vortices in other layers as the interlayer coupling becomes weaker, thereby enhancing the noise power.

I. INTRODUCTION

Due to their inherent materials characteristics such as high-transition temperature, short-coherence length, large anisotropy, etc, high-T_c cuprate superconductors (HTSC's) are well known to have very complicated vortex phase diagrams.[1] In particular, large anisotropy, thought to originate mainly from the layered crystal structures, gives rise to a further complexity in the vortex dynamics. As the anisotropy increases, we should consider the interlayer interaction between vortices in different layers as well as the in-plane interaction. Thus, HTSC's have been investigated extensively from the viewpoint of the phase transition in a quasi-two-dimensional (2D) system. In an extreme 2D case, the superconducting transition can be described by the famous Kosterlitz-Thouless (KT) theory.[2] Evidences of vortex-antivortex unbinding transition behavior have been observed by many research groups in $YBa_2Cu_3O_{7-\delta}$ (YBCO) system[3] as well as in bismuthates[4] from the early stage of HTSC era. As more and more research efforts were made, it turned out that a better understanding of these phenomena requires more stringent treatment of these systems including the interlayer coupling. Thus, recently the role played by the interlayer coupling has been intensively studied. For example, Wan *et al.*[5] observed a sequential transition due to the interlayer coupling and KT unbinding of vortex-antivortex pairs from the measurement of zero-field resistive transition of Bi-2212 single crystals. More recently, Hellerqvist *et al.*[6] reported on the dynamic ordering induced by the transport current in 2D amorphous $Mo_{77}Ge_{23}$ films. They found out that the ordering occurs when the current suppresses the pinning potential sufficiently and that stiffening of the lattice by increasing either the film thickness or the applied field reduces the current density required to bring about the ordering.

As the technology of thin film fabrication developed, it became possible to make artificial structures having various anisotropy. Thus, by using synthesized HTSC superlattices we can probe the intermediate regime, that is, the regime between moderately anisotropic YBCO system and extremely anisotropic Bi-Sr-Ca-Cu-O system.[7–12] Many experiments on the vortex dynamics in these artificial structures have been carried out with measurements of typical transport properties such as resistivity, current-voltage characteristics, Hall effect, etc.[13–15] Although it is well known that noise measurement can enhance our understanding of dynamical systems, there has not been done much systematic study on the noise properties of a vortex system in HTSC superlattices with varying coupling strength.[16] So, in this study, we focused on the measurement of noise properties related to the vortex motion in a series of HTSC $YBCO/PrBa_2Cu_3O_{7-\delta}(PBCO)$ superlattices with different modulations. The noise peak power showed a nonmonotonic dependence on the transport current in a given system, while it decreased monotonously with increasing magnetic field. We also observed that the maximal noise peak power and the corresponding current value simultaneously increased with the decrease of coupling strength. We could understand these behaviors by considering a dynamic ordering of vortices.

II. EXPERIMENT

We have grown superlattice thin films by dc magnetron sputtering with compound targets. The detailed process is depicted elsewhere.[17] Briefly describing, the deposition temperature was about 750 °C and the partial pressures of Ar and O_2 gases were 60 mTorr for YBCO, 40 mTorr for PBCO, respectively. Firstly, 200 Å-thick PBCO was depos-

ited as a template layer. Each of YBCO and PBCO layers with desired thickness was deposited by rotating the substrate heater block to each sputter gun and subsequently sputtering for a predetermined time. This process was repeated 10 - 15 times. The terminating layer was always 100 Å-thick PBCO layer to passivate the whole structure. Superlattice modulations were such as $(YBCO)_8/(PBCO)_n$ with n equal to 2, 4, and 8. After the deposition finished, films were *in-situ* annealed at about 450 °C under the oxygen atmosphere of 600 Torr for about an hour.

From the x-ray diffraction analysis, we could not observe any peak other than $(00l)$ peaks and satellite peaks on both sides of them, indicating a c-axis texturing. Calculated c-axis lattice parameter was 11.7 Å, in agreement with the reported value. Satellite peaks were ascribed to the superlattice modulation, whose wavelength calculated from the separation of satellite peaks was in accordance with the expected value. From the atomic force microscopy analysis of single-layer films, we found out that PBCO layer grows more smoothly compared to other layers with the rms roughness of about 5 Å in 4 μm$\times$4μm area, which is an extremely small value. It was about 30 Å for YBCO layer of equal size. As can be expected from these rms values, the thicker the intervening PBCO layer becomes, the better the surface smoothness. The rms value of $(YBCO)_8/(PBCO)_8$ in an equal area is about 8 Å, which is comparable to that of PBCO.

For the measurement of transport properties of superlattice thin films, we patterned them into a Hall bar geometry using techniques of photolithography and ion milling. The linewidth was 200 μm and the distance between voltage leads was 4 mm. To reduce the contact resistance and to ensure a uniform current flow, we formed contact pads with gold layer covering edges as well as top surfaces. We attached lead wires using an indium soldering or a wire bonding. The typical contact resistance was smaller than 1 Ω at temperature below T_c. Transport measurements were done by the four-probe method. The noise measurements were performed by the standard lock-in technique using an EG&G model 5302 lock-in amplifier of Princeton Applied Research in the noise mode. A bias current was applied by a homemade battery current source to exclude any external noise due to ac sources. The frequency of lock-in amplifier was set at 17 Hz in this study to avoid any existing harmonics and subhamonics of the 60-Hz noise. A further information on the vortex dynamics may be obtained by the measurement of noise power spectrum, which will be a future extension of current study. We measured noise as a function of temperature, depending on the transport current and the magnetic field. The applied transport current ranges from 10 μA to 1 mA. External magnetic field was applied perpendicularly to both the current and the film plane up to 160 G using an electromagnet.

III. RESISTIVE TRANSITION

Temperature dependence of the resistivity is plotted in Fig. 1. The electrical conductivity shows metallic but somewhat disordered behavior in the normal states. This implies that there might exist some defects such as the mixing between YBCO and PBCO layers. To clarify the origin, we calculated resistivity using the form $\rho=Rwd/l$, where d is

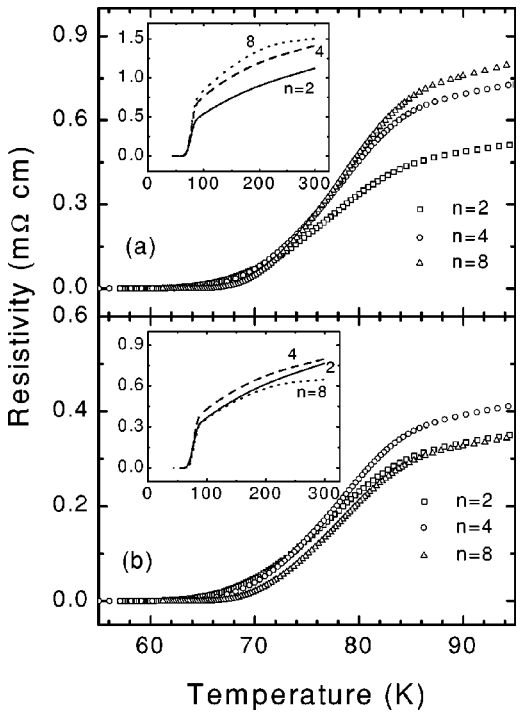

FIG. 1. Temperature dependence of the resistivity of $(YBCO)_8/(PBCO)_n$ superlattices. Resistivity is calculated from the measured resistance data using the relation $\rho=Rwd/l$, where w,d,l is the width, thickness, and length of the sample. Curves in (a) and (b) are when d is taken as the total thickness and the sum of thicknesses of YBCO layers, respectively.

the total thickness of the sample in Fig. 1(a) and the sum of thicknesses of YBCO layers in Fig. 1(b). While the curves in Fig. 1(a) show substantial discrepancies, they come closer to each other in Fig. 1(b). By simplifying the superlattice structure as a parallel resistor model (alternating YBCO and PBCO resistors), we can calculate the resistivity using the form, $d/\rho=d_Y/\rho_Y+d_P/\rho_P$, where d_Y (d_P) and ρ_Y (ρ_P) are the thickness and the resistivity of YBCO (PBCO) layer, respectively. Resultant resistivity curves fall between those in Fig. 1(a) and in Fig. 1(b). If the interface does not play a significant role in the electrical conduction, these curves should come closer to those in Fig. 1(b) than to those in Fig. 1(a), since the transport current will flow dominantly along the YBCO layers instead of along the semiconducting PBCO layers. Thus, we can conjecture that the interface layer contributes some portion to the electrical conduction through the scattering of charge carriers or intermixing of YBCO and PBCO layers, or any others. This is not in accordance with the result of Wang *et al.*[18]

In the superconducting transition region, resistivity curves of three specimens show almost the same behavior. That is, transition onset temperatures ($T_{c,\mathrm{on}}$) are nearly equal, i.e., about 85 K, although the zero-resistance temperature scatters a little. Assuming that the overall electrical transport in the three samples might be due to the same mechanism, we tried to explain the resistive transition using a single unified model. To begin with, smoothing of a resistivity curve around $T_{c,\mathrm{on}}$ is reminiscent of the conductance enhancement due to fluctuations in the amplitude of order parameter, which was described well by Aslamazov and Larkin.[19] The theoretical form is given as

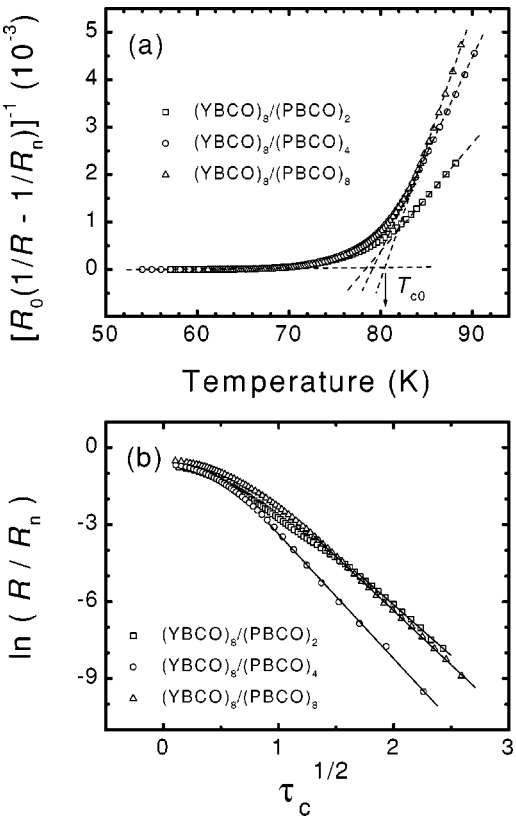

FIG. 2. Fitting of the sheet resistance to (a) the conductance fluctuation model by Aslamazov-Larkin and (b) the form $R/R_n \sim \exp[-2(b\tau_c)^{1/2}]$, which is predicted by the combination of the Kosterlitz-Thouless theory and Bardeen-Stephen flux-flow model. In (a) we can see that the fitting is rather satisfactory and gives a nearly identical fitting parameter of T_{c0}, i.e., ~ 79 K and in (b) the solid lines denote the well-fitted ranges.

$$\frac{1}{R}=\frac{1}{R_n}+\frac{1}{R_0(T/T_{c0}-1)}, \tag{1}$$

where R_n is the normal state sheet resistance, $R_0=16\hbar/e^2=6.58\times10^4\ \Omega/\square$, and T_{c0} is the BCS mean-field transition temperature. Instead of using the predicted value of R_0, we performed two-parameter fitting by varying both R_0 and T_{c0}. Figure 2(a) shows the sheet resistance fitted to Eq. (1). Linear extrapolation from both sides of the transition gives birth to T_{c0} of 79 K, which highly deviates from the value of 85 K (See Table 1.)

As for the mechanism of resistance curve broadening, we conjectured that flux flow due to the unbinding of vortex-antivortex pairs might be a relevant one. According to the KT theory,[2] pre-formed vortex-antivortex pairs start to dissociate by thermal fluctuations at the KT transition temperature, T_{KT}. These free vortices will generate dissipation above T_{KT} when acted on by the transport current. Neglecting the pinning, the resistance due to a free-flux motion is given by the Bardeen-Stephen theory.[20] On the other hand, according to Helperin and Nelson[21], the temperature dependence of free vortex (antivortex) density, N_+ (N_-), is given by

$$N_+=N_-\approx\frac{1}{2\xi_{ab}^2}\exp\left[-2\sqrt{b\frac{T_{c0}-T}{T-T_{KT}}}\right]. \tag{2}$$

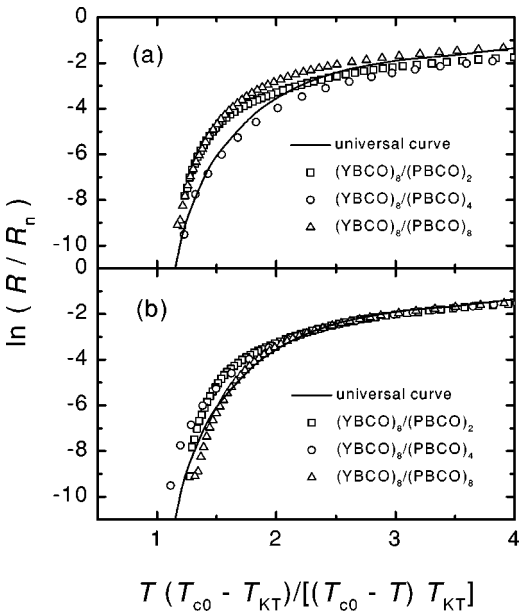

FIG. 3. Scaling of the sheet resistance by the two-dimensional Coulomb gas model. Curves in (a) are obtained by using T_{KT} values from the KT fitting, and in (b) by taking T_{KT} and T_{c0} as free parameters. We can see that the latter gives better results.

Thus, we can write the flux-flow resistance as

$$R=2\pi\xi_{ab}^2(N_++N_-)R_n=2\pi R_n\exp\left[-2\sqrt{b\frac{T_{c0}-T}{T-T_{KT}}}\right], \tag{3}$$

where R_n is the normal state resistance, b is a constant of order unity, and $\xi_{ab}=12$ Å is the coherence length along the a-b plane. Using R_n and T_{c0} values obtained from the above resistance fitting to conductance fluctuations, we tried to fit the sheet resistance to Eq. (3), taking T_{KT} and b as free parameters. The results are displayed in Fig. 2(b). We can see that fitting is good only in the limited temperature range near the zero-resistance temperature. Well-fitted temperature range differs from sample to sample and is indicated by solid straight lines.

Noting the limitation of the KT theory, Minnhagen pointed out that resistance prediction based on the ''asymptotic'' Kosterlitz renormalization-group equations is valid only over a small temperature interval compared to the width of the resistive transition.[22,23] He developed a universal scaling theory for the resistance of a 2D superconductor, starting from the analogy between 2D Coulomb gas and vortices in a 2D superconductor. According to this theory, the resistance should be scaled by a universal temperature parameter, $X=T(T_{c0}-T_{KT})/(T_{c0}-T)T_{KT}$. Thus, we again tried another fitting of normalized sheet resistance. The results are shown in Fig. 3. Figure 3(a) is the result obtained using parameters from the previous fittings and Fig. 3(b) by taking T_{KT} and T_{c0} as free parameters. We can see that the scaling is more satisfactory when we take T_{KT} and T_{c0} as free parameters. Fitting parameters are given in Table I. In an ideal case of a strictly 2D superconductor, the curves should converge to a single universal curve,[22] which is displayed as a continuous line in the figure. A slight deviation in the figure indicates that these specimens do not behave as a strictly

TABLE I. Characteristic parameters of $(YBCO)_8/(PBCO)_n$ superlattice samples. $T_{c,on}$ is the onset temperature estimated from the linear extrapolation from both sides of the transition and $T_{c,zero}$ is the zero-resistance temperature. T_{c0} is the BCS mean-field transition temperature with T_{c0}^{AL} obtained from the fitting using the Aslamazov-Larkin theory of conductance fluctuation, T_{c0}^{M} from the universal scaling of Minnhagen, and T_{c0}^{IV} from $I-V$ curves. T_{KT} is the Kosterlitz-Thouless transition temperature with T_{KT}^{RT} obtained from the flux-flow resistance fitting, T_{KT}^{IV} from $I-V$ curves, and T_{KT}^{M} from the universal scaling of resistance. R_ns are the normal state sheet resistances and R_0s are fitting parameters to the conductance fluctuation model. b is the parameter of order unity in the KT fitting.

	$(YBCO)_8/(PBCO)_2$	$(YBCO)_8/(PBCO)_4$	$(YBCO)_8/(PBCO)_8$
$T_{c,on}$(K)	84.6	84.8	84.5
T_{c0}^{AL}(K)	78.5	79.2	80.5
T_{c0}^{M}(K)	79.5	79.8	78.5
T_{c0}^{IV}(K)	62.5	59.1	65.3
$T_{c,zero}$(K)	59.9	59.8	64.1
T_{KT}^{RT}(K)	57.3	56.5	62.2
T_{KT}^{IV}(K)	58.4	56.2	62.2
T_{KT}^{M}(K)	56.4	58.8	62.2
$R_n(\Omega/\square)$	27.00	39.45	39.50
$R_0(\Omega/\square)$	1350	2250	2250
b	3.71	6.48	4.64

2D superconductor. We conjecture that the interlayer coupling might play a role, thus we should take these systems as quasi-2D superconductors. In fact, a closer look at Fig. 3(b) shows that the deviation increases as the intervening PBCO layer gets thinner. Therefore, the dynamics of vortices in our specimens can be understood only if we take into account the effect of interlayer coupling as well as the intervortex interaction and the vortex-pinning potential interaction.

IV. CURRENT-VOLTAGE CHARACTERISTICS

Another feature of vortex unbinding transition is a universal jump of exponent in current-voltage ($I-V$) characteristics. According to the KT theory, $I-V$ curves at temperatures lower than T_{KT} show a power-law behavior of the form $V\sim I^{1+\pi K}$. Here, at $T=T_{KT}$ the reduced Kosterlitz-Thouless stiffness constant K is given by

$$K=\frac{2}{\pi}=\frac{\pi\hbar^2 n_s^0}{4m^* k_B T_{KT}\epsilon_c}, \tag{4}$$

where m^* is the effective mass of carriers, n_s^0 is an unrenormalized 2D superfluid carrier density, and ϵ_c is an effective dielectric constant representing the screening strength between vortex pairs. Thus, it follows that the exponent of power-law $I-V$ curves should show an abrupt jump down from 3 to 1 with increasing temperature.

$I-V$ curves at around and below T_c are plotted in a logarithmic scale in Fig. 4. We can see that three data sets are quite similar qualitatively with only a slight difference in detail. While $I-V$ curves are linear in the high-temperature region, at low temperature there appears a nonlinear part in the high-current limit. This part becomes longer with decreasing temperature as the linear region shrinks nearly to zero at a certain temperature. This phenomenon can be understood by the fact that besides the thermal unbinding vortex-antivortex pairs can also be dissociated by the transport current larger than the threshold one (I_{th}) since the Lorentz force acts oppositely on each partner of a pair. Fiory *et al.*[24] argued that this threshold current could be estimated by

$$I_{th}=\frac{2eK(l_W)k_BT}{\hbar}, \tag{5}$$

where $K(l)$ is the Kosterlitz-Thouless reduced stiffness constant, and $l_W=\ln(W/\xi_{core})$ is an experimental length parameter for a sample of width W and vortex-core size ξ_{core}. By taking $\xi_{core}\sim 12$ Å, the in-plane Ginzburg-Landau coherence length at T_{KT}, and $W=200$ μm in our case, we get $l_W\approx 12.0$. Approximating $K(l)$ at large l by $K(l)\approx(1/\pi)(2+l^{-1})$ (valid at $T=T_{KT}$), we obtain $I_{th}\approx 1.67$ μA for our samples. This value is larger by one order of magnitude than that of Garland *et al.*'s estimation[25] in composites of indium and indium oxide. In our case, the nonlinearity appears when the current exceeds the value ~ 1 μA at $T=60$ K in Fig. 4(a), in agreement with the estimated value. Thus, we can confirm that this simple estimation of the threshold current further corroborates the vortex-unbinding picture. Figure 5 shows the temperature dependence of the exponent in $I-V$ curves in the low-current limit. Although the appearance of universal jump is not clear, the curves show some evidences of the involvement of vortex fluctuations. We identify the temperature where the exponent becomes 3 as the KT transition temperature. T_{KT} obtained from this scheme is compared with those from the resistance fitting in Table I. We can see that they are consistent with each other. Outside the critical region below T_{KT}, the superfluid density varies linearly to the reduced temperature as $n_s^0\sim 1-T/T_{c0}$. So, we conjecture that it can be possible to estimate T_{c0} by extrapolating the linear region down to $1+\pi K(T_{c0})=1$, as in the reports by Kadin *et al.*[26] and Garland *et al.*[25] The estimated values of T_{c0} are 62.5, 59.1, and 65.3 K, respectively. These do not agree with those obtained from the resistance curves. We consider that these deviations may be related to the interlayer coupling.

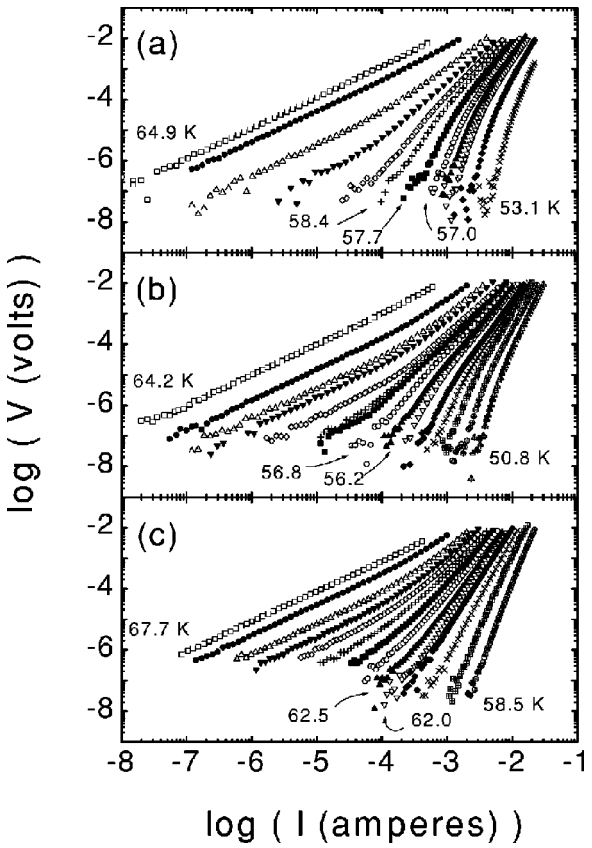

FIG. 4. Current-voltage characteristics of $(YBCO)_8/(PBCO)_n$ superlattices. Each curve was obtained at constant temperatures. In (a), $n=2$ and temperatures are 64.9, 62.9, 60.6, 59.6, 58.9, 58.4, 57.7, 57.0, 56.5, 56.0, 54.9, and 53.1 K. $n=4$ in (b) and they are 64.2, 61.4, 59.8, 59.1, 58.2, 57.7, 57.4, 56.8, 56.2, 55.6, 55.0, 54.3, 53.3, 52.1, and 50.8 K. In (c), $n=8$ and they are 67.7, 66.6, 65.6, 65.0, 64.5, 64.0, 63.5, 63.0, 62.5, 62.0, 61.7, 60.9, 59.8, and 58.5 K.

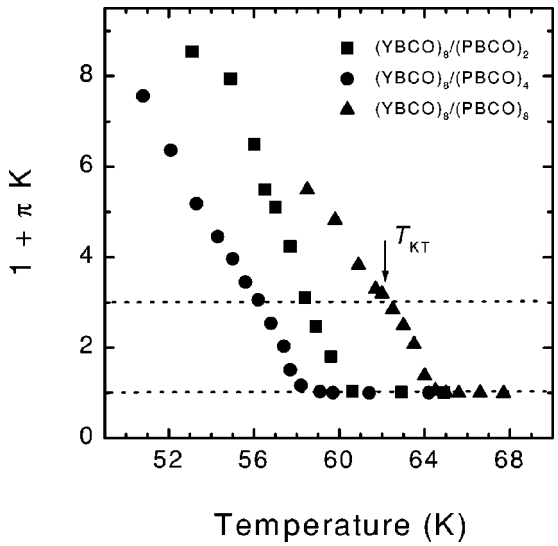

FIG. 5. Exponent of $I-V$ curves in the form of power-law $V \sim I^{1+\pi K}$. The exponents are determined in the low current limit. We can observe a jump down of the exponent as the temperature is increased. The temperature where the exponent becomes 3 is identified as the Kosterlitz-Thouless transition temperature.

V. NOISE PROPERTIES

Noise measurements can enhance our understanding for the transport phenomena in HTSC's.[27–37] Although much interest for the study of interlayer coupling has been drawn recently, there have not been many reports on noise measurements related to the vortex dynamics affected by the interlayer interaction. To study this effect, we measured the temperature dependence of the noise power spectral density in a series of HTSC superlattices with varying strength of interlayer coupling. In the normal state, we observed no significant features except the thermal noise, which is often called Johnson noise and originates from the fluctuation of sample resistance.

Figure 6 shows how the noise power evolves in the transition regime as the current increases. There are some noticeable features common to all the data. Firstly, as the temperature is lowered, the noise power appears far below 78 K, where the derivative of resistance (dR/dT) is maximal, which is in contrast with other reports that the noise peak appears where dR/dT is maximal.[29] Thus, we can exclude a resistance fluctuation mechanism as a major source of the noise. In fact, the noise peak appears near the tail part of resistance curve. The temperature where the noise power culminates does not scatter so much within our experiments.

As for the current dependence, it is a common behavior in our three specimens that the noise peak becomes broad and stronger up to a certain critical current, which we denote as I_p, but it gets weaker above I_p. The noise power was not enhanced for a current larger than a second critical one, which we designate as I_d. For the qualitative explanation of this, to begin with, recall that we could describe the resistive

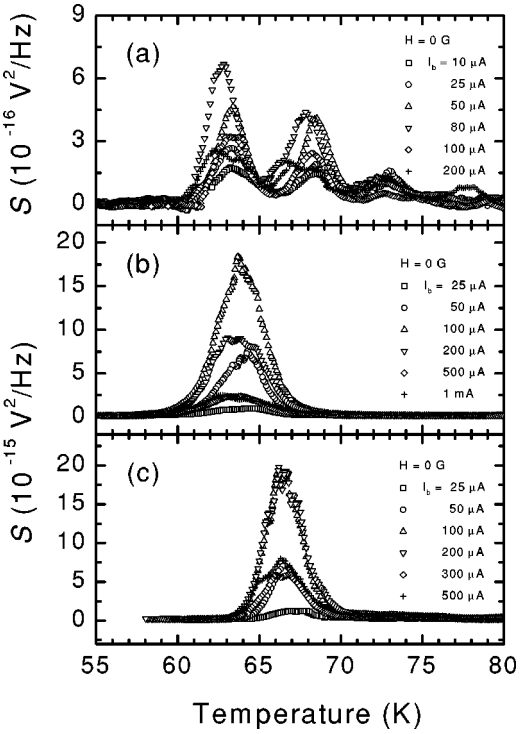

FIG. 6. Spectral density of the noise power of $(YBCO)_8/(PBCO)_n$ superlattices as a function of temperature when the transport current is varied. $n=2$, 4, and 8 in (a), (b), and (c), respectively. The pick-up frequency is fixed to 17 Hz and the magnetic field is not applied.

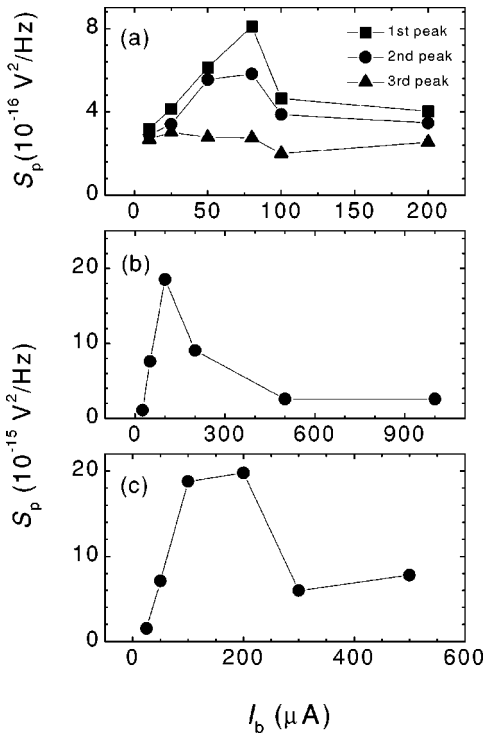

FIG. 7. Current-dependence of the noise peak power in each curve in Fig. 6. The noise peak power shows a nonmonotonic behavior.

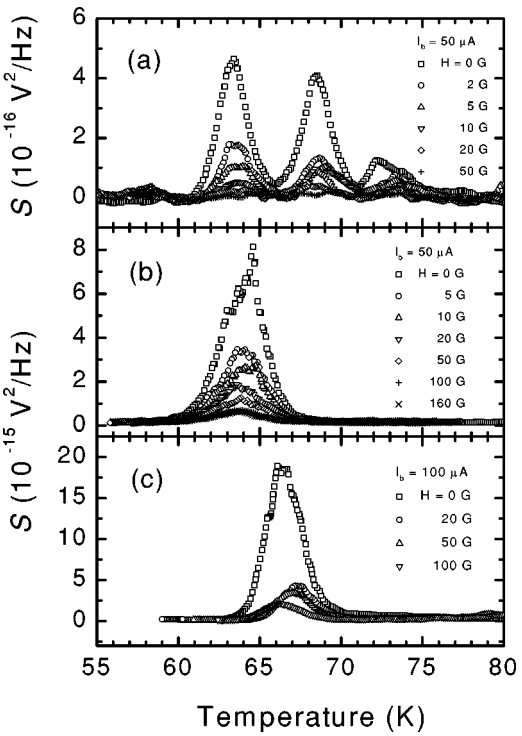

FIG. 8. Spectral density of the noise power $(YBCO)_8/(PBCO)_n$ superlattices as a function of temperature when the magnetic field is varied. $n=2$, 4, and 8 in (a), (b), and (c), respectively. The pick-up frequency is fixed to 17 Hz and the current value is indicated in the figure.

transition and current-voltage characteristics based on the theories of vortex fluctuation. Vortex unbinding by thermal fluctuations will occur completely at T_{KT}, when there exists a mixture of free vortices and antivortices in equilibrium. Most of free vortices and antivortices will stay at pinning sites under no applied current. In this case, no noise except the thermal one can be detected. Applying a driving current to the sample, we can move them unless the driving force is smaller than the pinning force. Because the driving force is acted on them oppositely, they will move in opposite directions. However, the induced emfs by moving vortices and antivortices are added in the longitudinal direction, although they are canceled in the transverse component. So, we can expect that the longitudinal voltage drop will be enhanced if the current is increased. For a current smaller than I_p, we observed an enhancement of noise with increasing current. This can be explained if we think that vortices and antivortices are moving more randomly until a steady flux flow is established. A current larger than I_p will prevent them from moving chaotically, so a more or less ordered state is achieved. Thus, the noise peak will be suppressed until a saturation is reached at $I=I_d$. This phenomenon is summarized in Fig. 7, where we plot the noise peak power (S_p) for each current value. We can also see that the maximal noise peak power and the corresponding current increases with increasing PBCO layer thickness.

The dynamics of vortices in a layered superconductor will be influenced by the interlayer coupling as well as by the intervortex interaction. In this respect, we noticed Hellerqvist *et al.*'s report[6] on the current-induced ordering of vortices in 2D $Mo_{77}Ge_{23}$ films. According to them, the ordering occurs when the intervortex interaction dominates the disorder potential. They also argued that stiffening of the vortex lattice by increasing either the film thickness or the applied field reduces the current density required to bring out the dynamic ordering. We can explain our noise data by a simple analogy. Firstly, the superlattice sample can be regarded to have a smaller anisotropy as the intervening layer gets thinner. This means that vortices will behave as flux lines in $(YBCO)_8/(PBCO)_2$, while they can be taken as pancakelike in $(YBCO)_8/(PBCO)_8$. Therefore, vortices in each YBCO layer of a superlattice will move more correlatedly as the PBCO layer gets thinner. In this case, dynamic ordering can be brought about by a rather small current. On the other hand, if the correlation between vortices in different layers gets weaker, relatively large current is required to induce a dynamic ordering. Interpreting the noise power in terms of dynamic ordering of vortices, we can consider a one-to-one correspondence between the extent of ordering and noise power. The increase of maximal noise peak power with increasing PBCO layer thickness is naturally explained using the above arguments. Namely, large randomness of vortex motion is expected when the vortex becomes 2D in nature, whence a large noise power is resulted. Another point to explain is the multiple peaks appearing only in $(YBCO)_8/(PBCO)_2$. We believe the peaks accompanying the main one near 65 K might originate from some inhomogeneities in the sample. For example, mixing between YBCO and PBCO layers in the interface region can give rise to local fluctuations of T_c.

Now let us turn to the field dependence of the noise power, which is plotted in Fig. 8. In contrast to the current dependence, we found out that the noise behavior with a magnetic field shows a monotonous trend, i.e., the noise

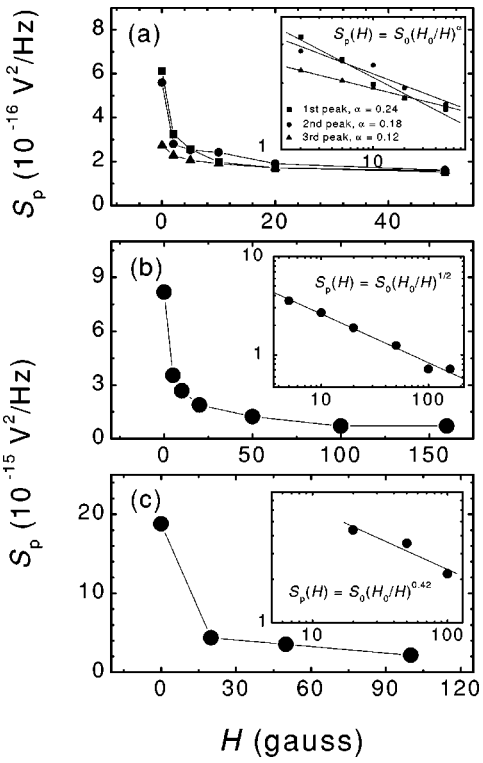

FIG. 9. Field dependence of the noise peak power in each curve in Fig. 8. We observe that the noise peak power is suppressed monotonically as the field is increased. Inset: fitting of the noise peak power to a power-law form $S_p = S_0(H_0/H)^\alpha$. α differs from sample to sample.

peaks get suppressed as the field is increased. This is common to all the investigated samples, and clearly visible in Fig. 9, where we plotted the noise peak power versus the magnetic field. In fact, there have been some reports of a monotonous decrease of noise subjected to a magnetic field.[30–32] Voss *et al.* measured noise of aluminum and tin films as a function of current and field.[30,31] They ascribed the noise reduction by the magnetic field to the decrease of mean free path, therefore the reduced phase slip giving a suppressed noise power.

The applied magnetic field increases the total number of free vortices and antivortices by reducing the effective KT transition temperature, while introducing the fixed difference in the number density, i.e., $N_+ - N_- = B/\Phi_0 \approx H/\Phi_0$. Here, recall that we could describe the resistive transition using the flux-flow models. Then, as described in the above, these free vortices and antivortices will give rise to the voltage noise in the longitudinal direction. At first, let us consider the case of weak interlayer coupling, where we have only to consider the in-plane interaction, although there are additional interactions between dissociated vortex-antivortex pairs and field-induced vortices as well as the effects of pinning and interlayer coupling. The interaction is expected to increase monotonously as the magnetic field (hence the vortex density) is increased. Then, vortices will move collectively rather than independently. As a result, the dynamic ordering could be established more easily than in the case of an independent motion. Thus, we can expect that noise will be suppressed for a given current if the magnetic field is increased, as is evident in Fig. 9.

The suppression rate of noise peak power may be related to the interlayer coupling strength and is different depending on it. We tried to estimate it by fitting the data to a functional form of $S_p(H) = S_0(H_0/H)^\alpha$, and the results are shown in the insets of Fig. 9. The exponent, α, is 0.24 (for the main peak), 0.5, and 0.42 for $n=2$, 4, and 8 in $(YBCO)_8/(PBCO)_n$. A noticeable feature for $(YBCO)_8/(PBCO)_2$ sample is that α decreases linearly as we move to the peak at a higher temperature. This implies that the noise suppressions may be due to different mechanisms, although it may involve the vortex interaction basically. When the interlayer interaction is strong enough, entities giving a voltage drop (hence noise) are flux lines. Meanwhile, pancake vortices will induce the electromotive force if the interlayer coupling is weak. In this case, maximal noise peak power is resulted when the randomness of pancake vortex motion is maximized. The suppression rate will be determined by the competition between intervortex interaction in the same plane and in different planes. More study, including a simulation of vortex motion, is required for a more quantitative understanding.

VI. CONCLUSIONS

Through the measurement of resistivity and current-voltage characteristics in a series of HTSC YBCO/PBCO superlattices with varying coupling strength, we have found out that the superconducting transition could be described by vortex fluctuation theories considering the interlayer coupling. Noise measurements revealed that the noise in the transition region is originated from the vortex motion instead of conductance fluctuations. The noise peak power showed a nonmonotonic dependence on the transport current, while it decreased monotonously with increasing magnetic field. In addition, the maximal noise peak power and the corresponding current increases simultaneously with decreasing interlayer coupling. We have shown that these behaviors could be explained in terms of dynamic ordering of vortices by taking into account both the in-plane and interlayer vortex interactions

ACKNOWLEDGMENTS

This work was supported by the Ministry of Science & Technology in Korea. We would like to acknowledge Su-Youn Lee for the skillful assistance in the photolithography process.

[1] G. Blatter, M. V. Feigel'man, V. B. Geshkenbein, A. I. Larkin, and V. M. Vinokur, Rev. Mod. Phys. **66**, 1125 (1994), and references therein.
[2] J. M. Kosterlitz and D. J. Thouless, J. Phys. C **6**, 1181 (1973); J. M. Kosterlitz, *ibid.* **7**, 1046 (1974).
[3] Y. Matsuda, S. Komiyama, T. Onogi, T. Terashima, K. Shimura, and Y. Bando, Phys. Rev. B **48**, 10 498 (1993); Y. Kopelevich, F. Ciovacco, P. Esquinazi, and M. Lorenz, Phys. Rev. Lett. **80**, 4048 (1998).
[4] S. Martin, A. T. Fiory, R. M. Fleming, G. P. Espinosa, and A. S. Cooper, Phys. Rev. Lett. **62**, 677 (1989); A. K. Pradhan, S. J. Hazell, J. W. Hodby, C. Chen, Y. Hu, and B. M. Wanklyn, Phys. Rev. B **47**, 11 374 (1993); L. Miu, P. Wagner, U. Frey, A. Hadish, Dana Miu, and H. Adrian, *ibid.* **52**, 4553 (1995); L. Miu, G. Jakob, P. Haibach, Th. Kluge, U. Frey, P. Voss-de Haan, and H. Adrian, *ibid.* **57**, 3144 (1998).
[5] Y. M. Wan, S. E. Hebboul, D. C. Harris, and J. C. Garland, Phys. Rev. Lett. **71**, 157 (1993); Y. M. Wan, S. E. Hebboul, and J. C. Garland, *ibid.* **72**, 3867 (1994).
[6] M. C. Hellerqvist, D. Ephron, W. R. White, M. R. Beasley, and A. Kapitulnik, Phys. Rev. Lett. **76**, 4022 (1996); M. C. Hellerqvist and A. Kapitulnik, Phys. Rev. B **56**, 5521 (1997).
[7] Z. Z. Li, H. Rifi, A. Vaures, S. Megtert, and H. Raffy, Phys. Rev. Lett. **72**, 4033 (1994).
[8] I. Bozovic and J. N. Eckstein, J. Supercond. **8**, 537 (1995).
[9] R. G. Goodrich, P. W. Adams, D. H. Lowndes, and D. P. Norton, Phys. Rev. B **56**, R14 299 (1997).
[10] I. Bozovic and J. N. Eckstein, in *Physical Properties of High Temperature Superconductors*, edited by D. M. Ginsberg (World Scientific, Singapore, 1996), Vol. 5.
[11] L. M. Wang, H. C. Yang, and H. E. Horng, Phys. Rev. Lett. **78**, 527 (1997).
[12] B. Zhao, F. Ichikawa, T. Fukami, T. Aomine, J.-J. Sun, B. Xu, and L. Li, Phys. Rev. B **55**, 1247 (1997).
[13] D. Norton and D. H. Lowndes, Phys. Rev. B **48**, 6460 (1993).
[14] M. Rasolt, T. Edis, and Z. Tešanović, Phys. Rev. Lett. **66**, 2927 (1991).
[15] Y. Matsuda, S. Komiyama, T. Terashima, K. Shimura, and Y. Bando, Phys. Rev. Lett. **69**, 3228 (1992).
[16] C. T. Rogers, K. E. Myers, J. N. Eckstein, and I. Bozovic, Phys. Rev. Lett. **69**, 160 (1992).
[17] W. K. Park, S. Y. Lee, and Z. G. Khim, in *Superconducting Superlattices II: Native and Artificial*, *Proceedings of the International Society for Optical Engineering, San Diego, California*, edited by I. Bozovic and D. Pavuna (SPIE, Bellingham, 1998), Vol. **3480**, p. 77.
[18] L. M. Wang, H. C. Yang, and H. E. Horng, Phys. Rev. B **56**, 6231 (1997).
[19] L. G. Aslamazov and A. I. Larkin, Fiz. Tverd. Tela (Leningrad) **10**, 1104 (1968) [Sov. Phys. Solid State **10**, 875 (1968)].
[20] J. Bardeen and M. J. Stephen, Phys. Rev. **140**, A1197 (1965).
[21] B. I. Halperin and D. R. Nelson, J. Low Temp. Phys. **36**, 599 (1979).
[22] P. Minnhagen, Phys. Rev. B **23**, 5745 (1981); **24**, 6758 (1981); in *Proceedings of the NASI Conference on Percolation, Localization, and Superconductivity*, edited by A. M. Goldman and S. A. Wolf (Plenum Press, New York, 1984), p. 287.
[23] For a comprehensive review of this topic, see, e.g., P. Minnhagen, Rev. Mod. Phys. **59**, 1001 (1987).
[24] A. T. Fiory, A. F. Hebard, and W. I. Glasberson, Phys. Rev. B **28**, 5075 (1983).
[25] J. C. Garland and H. J. Lee, Phys. Rev. B **36**, 3638 (1987).
[26] A. M. Kadin, K. Epstein, and A. M. Goldman, Phys. Rev. B **27**, 6691 (1983).
[27] L. B. Kiss and P. Svedlindh, IEEE Trans. Electro. Devices **41**, 2112 (1994).
[28] M. J. Ferrari, M. Johnson, F. C. Wellstood, J. J. Kingston, T. J. Shaw, and J. Clarke, J. Low Temp. Phys. **94**, 15 (1994).
[29] D. H. Kim, W. N. Kang, Y. H. Kim, J. H. Park, J. J. Lee, G. H. Yi, T. S. Hahn, and S. S. Choi, Physica C **246**, 235 (1995).
[30] R. F. Voss, C. M. Knoedler, and P. M. Horn, in *Inhomogeneous Superconductors-1979*, edited by D. U. Gubser *et al*., AIP Conf. Proc. No. 58 (AIP, New York, 1980), p. 314.
[31] R. F. Voss, C. M. Knoedler, and P. M. Horn, Phys. Rev. Lett. **45**, 1523 (1980).
[32] A. L. Li and I. Shih, Appl. Surf. Sci. **92**, 461 (1996).
[33] H. Safar, P. L. Gammel, D. A. Huse, G. B. Alers, D. J. Bishop, W. C. Lee, J. Giapintzakis, and D. M. Ginsberg, Phys. Rev. B **52**, 6211 (1995).
[34] G. D'Anna, P. L. Gammel, H. Safar, G. B. Alers, D. J. Bishop, J. Giapintzakis, and D. M. Ginsberg, Phys. Rev. Lett. **75**, 3521 (1995).
[35] P. J. M. Wöltgens, C. Dekker, S. W. A. Gielkens, and H. W. de Wijn, Physica C **247**, 67 (1995).
[36] Y. Zhao, H. Zhang, G. D. Gu, S. H. Han, G. J. Russell, and N. Koshizuka, J. Phys.: Condens. Matter **9**, 7593 (1997).
[37] T. Tsuboi, T. Hanaguri, and A. Maeda, Phys. Rev. Lett. **80**, 4550 (1998).